

LOW-ALPHA OPERATION OF THE SLS STORAGE RING

N. P. Abreu, M. Böge, F. Müller, V. Schlott, H. C. Sigg, A. Streun, PSI, Villigen, Switzerland
 G. Amatuni, D. Gishyan, K. Manukyan, A. Sargsyan, CANDLE, Yerevan, Armenia

Abstract

Recently operation of the Swiss Light Source (SLS) storage ring at low momentum compaction factor α has been established. We will present an analysis of the longitudinal dynamics and of the injection process, and explain our method to ensure closed orbit stability. First experimental data from measurements of bunch length and coherent THz spectra will be shown.

INTRODUCTION

In normal operation, the bunch length in the SLS storage ring is about 16 ps rms (potential well distortion included). In standard 400 mA top-up user operation it is even increased to about 40 ps (bunch train average) by means of the 3rd harmonic Landau cavities. Short X-ray pulses of only 0.06 ps rms are provided by the SLS-FEMTO insertion, however at rather limited flux.

Some SLS users performing time resolved experiments demand for a substantial X-ray flux at a pulse length of a few ps rms. This mode would also be interesting for THz-experiments due to the high yield of coherent radiation.

LOW-ALPHA LATTICE

The SLS storage ring has a circumference of 288 m and is operating at 2.4 GeV at a minimum emittance of 5 nm. The lattice is composed of 12 straight sections of three different types (6×4 m, 3×7 m, 3×11 m) connected by 12 triple bend achromats (TBA). Variation of momentum compaction is achieved through negative dispersion in the centre dipoles of the TBAs. The optics tested was designed to provide a linear momentum compaction of $\alpha_1 = 5.3 \times 10^{-5}$ and an emittance of 13 nm. Tuning of the chromatic sextupoles allows variation of the quadratic momentum compaction α_2 while maintaining constant α_1 . Two lattice configurations for $\alpha_2 = 3.43 \times 10^{-3}$, and for $\alpha_2 = 1.84 \times 10^{-3}$ have been studied.

LONGITUDINAL DYNAMICS

The longitudinal equations of motion in the low-alpha mode in the absence of damping are the following

$$\dot{\varphi} = \omega_0 h (\alpha_1 \delta + \alpha_2 \delta^2)$$

$$\dot{\delta} = \frac{\omega_0 e V_{rf}}{2\pi E_0} (\sin(\varphi_s + \varphi) - \sin \varphi_s)$$

where $\omega_0 = 2\pi/T_0$ is the revolution frequency of the reference particle, h is the harmonic number and φ_s is the synchronous phase. The size and shape of the buckets are obtained from the corresponding Hamiltonian

$$H_0 = \frac{1}{2} h \omega_0 \alpha_1 \delta^2 + \frac{1}{3} h \omega_0 \alpha_2 \delta^3 + \frac{\omega_0 e V_{rf}}{2\pi E_0} (\cos(\varphi_s + \varphi) + \varphi \sin \varphi_s)$$

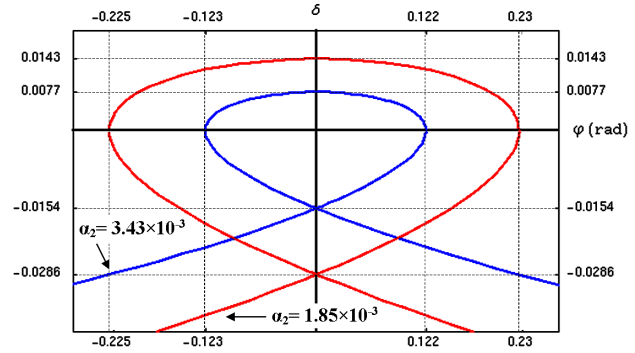


Figure 1: Alpha-buckets for $\alpha_1 = 5.3 \cdot 10^{-5}$ and two values of α_2 . Parameters of the SLS storage ring:

$$E_0 = 2.4 \text{ GeV}, h = 480, V_{rf} = 2.1 \text{ MV}, \varphi_s = 165^\circ$$

In low-alpha mode there are two different longitudinal phase space regimes depending on the value of the ratio $\alpha = \alpha_1/\alpha_2$, namely the RF-bucket and the alpha-bucket regime, which is shown in Fig. 1 for the two values of α_2 studied. For $\alpha_1 > 0$ and $\alpha_2 > 0$ (as it is the case for SLS) we have the RF-bucket regime for $\alpha > \sqrt{3} \cdot \delta_{linear}^{ac}$ and the alpha-bucket regime for $\alpha < \sqrt{3} \cdot \delta_{linear}^{ac}$.

$$\delta_{linear}^{ac} = \sqrt{\frac{e V_{rf} ((\pi - 2\varphi_s) \sin \varphi_s - 2 \cos \varphi_s)}{\alpha_1 \pi E_0 h}}$$

is the energy acceptance in the linear case (i.e. for $\alpha_2 = 0$).

INJECTION EFFICIENCY

In normal operation, the injection efficiency from the booster synchrotron to the SLS storage ring is close to 100%. In low-alpha mode however, the bunch coming from the booster synchrotron has an rms length of about 20 mm, or 67 ps, and cannot be captured completely by the low-alpha bucket. The maximum injection efficiency achievable thus is given by the integration of the injected bunch's particle distribution over the area of the low-alpha bucket. Fig. 2 shows the results as a function of α_2 for the design value of $\alpha_1 = 5.3 \times 10^{-5}$ and for the later measured (see below) value of $\alpha_1 = 3.6 \times 10^{-5}$.

These results were compared to TRACY simulations, tracking 25000 particles over 1500 turns. As an example, for the case of injecting a slightly longer bunch of 22 mm rms in the $\alpha_1 = 5.3 \times 10^{-5}$, $\alpha_2 = 3.4 \times 10^{-3}$ lattice, the tracking result of 39.5% confirmed the analytical value of 40.0%.

For the most studied optics at $\alpha_2 = 1.84 \times 10^{-3}$ the measured injection efficiency of 40% was close to the theoretical 45.6%, indicating a good lattice acceptance.

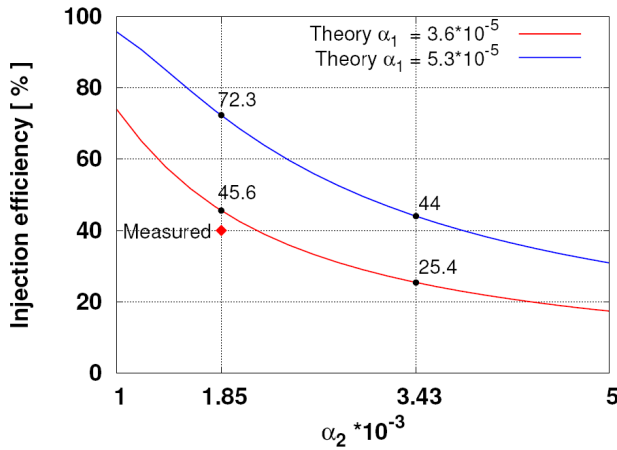


Figure 2: Theoretical injection efficiency as a function of α_2 for design (blue) and measured (red) value of α_1 .

ORBIT CORRECTION

The increase in length ΔC of the closed orbit due to a horizontal kick $\Delta x'_0$ at location “0” is given by

$$\Delta C \approx (\sqrt{\beta} b_0 \pi Q)^2 (\Delta x'_0)^2 / C_0, \quad b_0 = \sqrt{\beta_0} / (2 \sin \pi Q),$$

where we used the smooth approximation

$$\sqrt{\beta(s)} = \langle \sqrt{\beta(s)} \rangle =: \sqrt{\beta}, \quad \mu(s) = 2\pi Q s / C_0 \quad \text{and} \quad Q \gg 1.$$

The additional path length forces a change of closed orbit momentum δ to keep the length constant at $C_0 = h\lambda$,

$$\alpha_1 \delta + \alpha_2 \delta^2 + \frac{\Delta C}{C_0} = 0 \quad \xrightarrow{\Delta C \ll C_0} \quad \delta \approx -\frac{1}{\alpha_1} \frac{\Delta C}{C_0},$$

which is not negligible for low α_1 . The orbit thus is given as a superposition of the classical, linear orbit distortion, and a dispersive shrinkage (for $\alpha_1 > 0$) due to the reduction of momentum, which is quadratic in kick strength:

$$x(s) = \sqrt{\beta(s)} \cos \tilde{\mu}(s) \cdot (b_0 \Delta x'_0) - \frac{\eta(s) \sqrt{\beta}}{\alpha_1} \left(\frac{\pi Q}{C_0} \right)^2 (b_0 \Delta x'_0)^2$$

with $\tilde{\mu}(s) = \mu(s) - \mu_0 \pm \pi Q$, \pm for $s < s_0$, resp. $s > s_0$.

Thus the usual orbit correction scheme based on solution of a linear system faces convergence problems. We

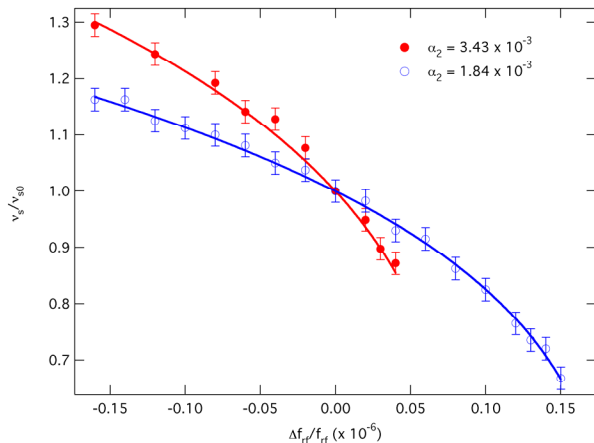


Figure 3: Measured synchrotron tune dependence with RF frequency change. The red and blue full lines are the fitting to the data.

determined δ from a SVD based dispersion fit to the horizontal orbit and calculated the required frequency shift for correcting the momentum utilizing the theoretical, and later the measured values for α_1 and α_2 . Applications of frequency shifts were alternated with corrections of the remaining orbit distortion (i.e. after subtracting dispersion) and iterated. It was necessary to reduce the granularity of the RF generator from 1.0 Hz to 0.1 Hz, and it helped to reduce the gain of the correction to avoid “overshooting” in frequency. Finally the fast orbit feedback system could be set into operation.

MEASUREMENTS

Measurement of α_1

In order to obtain the value of the first order momentum compaction factor we measured the variation of the synchrotron tune and mean orbit offset as a function of the RF frequency. In the analysis we used the calculated values of α_2 for the two different lattices and from the results we could estimate the value of α_1 . Fig. 3 shows the result of a scan of the synchrotron tune as a function of the RF frequency, to fit the data we used that [1]

$$\frac{\nu_s}{\nu_{s0}} = \left(1 - \frac{4\alpha_2}{\alpha_1^2} \frac{\Delta f_{RF}}{f_{RF}} \right)^{1/4}$$

and, Fig. 4 shows the result of a scan of the average orbit offset as a function of the RF frequency, in which the fitting function is given by

$$\langle \Delta x \rangle_{BPM} = -\frac{\langle \eta \rangle_{BPM} \alpha_1}{2\alpha_2} \left(1 - \sqrt{1 - \frac{4\alpha_2}{\alpha_1^2} \frac{\Delta f_{RF}}{f_{RF}}} \right)$$

From all four fittings it is possible to calculate $\alpha_1 = (3.6 \pm 0.2) \times 10^{-5}$, which is smaller than the calculated value of 5.3×10^{-5} .

Bunch Length Dependence on Current

The bunch length was measured as a function of the stored current per bunch for the two values of α_2 . The results are shown in Figure 5 where the green and red

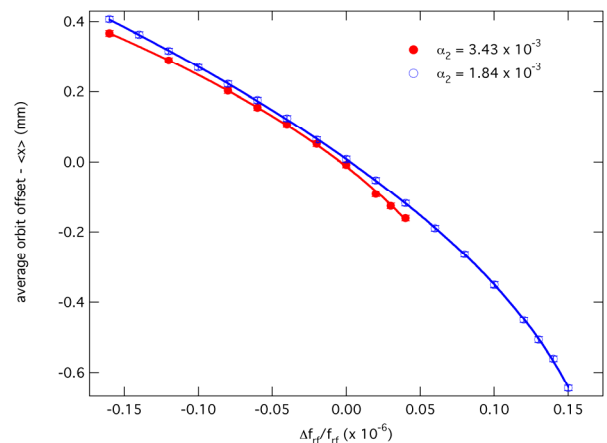


Figure 4: Measurement of the mean orbit deviation with RF frequency change. The red and blue full lines are the fitting to the data.

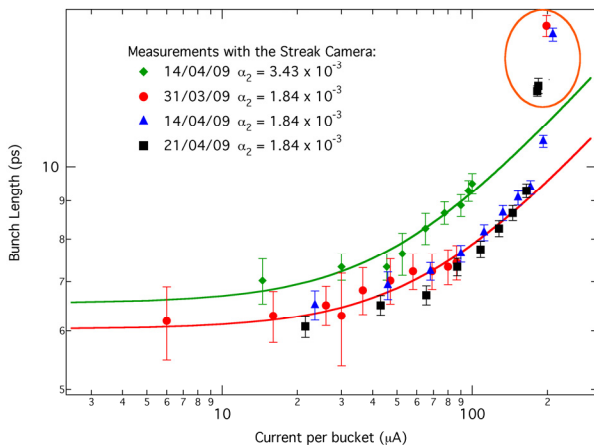


Figure 5: Bunch length as a function of the current per bucket. The green and red full line are the fitting of the 3/8 empirical power law to the data. For currents around 200 $\mu\text{A}/\text{bucket}$, for the case with smaller α_2 , the bunch length deviates from the empirical function as shown by the data points within the circle.

solid lines are the fitting of the data using the BESSY-II empirical formula in which $\sigma \propto I^{3/8}$ [2].

Notice that for both data sets the onset of bunch lengthening is about 50 $\mu\text{A}/\text{bucket}$, however bunches lengthen much faster for the case with $\alpha_2 = 3.44 \times 10^{-3}$ than $\alpha_2 = 1.84 \times 10^{-3}$. This dependence with α_2 is still not understood. The bunch length dependence with the current was also verified by observing the lifetime, which increases with increasing bunch length.

It is worth to observe also that the measured bunch length for low currents is around 6–6.5 ps which is not supported by measurements of the synchrotron tune ($f_s = 1.6$ kHz) that indicates a smaller bunch length closer to the predicted value of 4 ps. This discrepancy is probably due to some systematic error in the streak camera measurement, which has to be verified. Also, for currents close to 200 $\mu\text{A}/\text{bucket}$, corresponding to the case with $\alpha_2 = 1.84 \times 10^{-3}$ the bunch length gets much bigger than would be expected by using that $\sigma \propto I^{3/8}$, this is also accompanied by a increase in the THz intensity at higher wave numbers (see below).

Coherent THz-radiation

Spectra of coherent THz radiation have been taken at the infra-red (IR) beamline X01DC with a fast scan IR Fourier Transform spectrometer (Bruker 66) providing a spectral resolution of 1 cm^{-1} . The detector is a magnetically enhanced InSb hot electron bolometer with a sensitivity range up to 60 cm^{-1} (2 THz) and the measurement time was ≈ 200 s for 512 averages.

Normalized spectra for the series of 21/04/2009 (vide Fig.5) are shown in Fig.6. In order to be independent of the transfer function of the experimental set-up (incl. transfer line) we took an incoherent spectrum in normal user operation at ≈ 40 ps rms average bunch length for reference. There is virtually no transmission below 5 cm^{-1} (0.15 THz), so we see only the high frequency tail of the

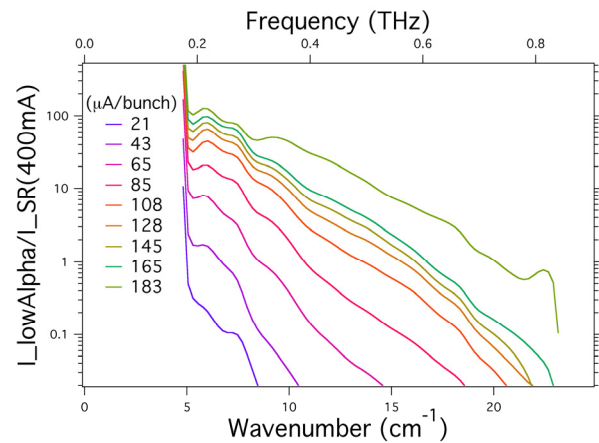


Figure 6: coherent THz spectra as a function of bunch current normalized to a spectrum measured in normal user operation at 400 mA and standard alpha of $\alpha_1 = 6 \times 10^{-4}$.

coherent radiation. The integrated intensity revealed a quadratic dependence on current up to 60 $\mu\text{A}/\text{bucket}$, above it became super-quadratic. For the maximum current, where the spectrum contains more intensity at higher frequencies, we observed bursting as shown in Fig. 7: the bursts appear at the synchrotron frequency of the low alpha mode of 1.681 kHz.

CONCLUSIONS AND OUTLOOK

We established a mode for low-alpha operation of the SLS storage ring with $\alpha_1 = 3.6 \times 10^{-5}$ including top-up injection and fast orbit feedback. The results on bunch length and THz spectra are only preliminary and require better understanding of the experimental set-ups and further investigation of the variation of bunch length and THz spectrum with bunch current and the value of α_1 .

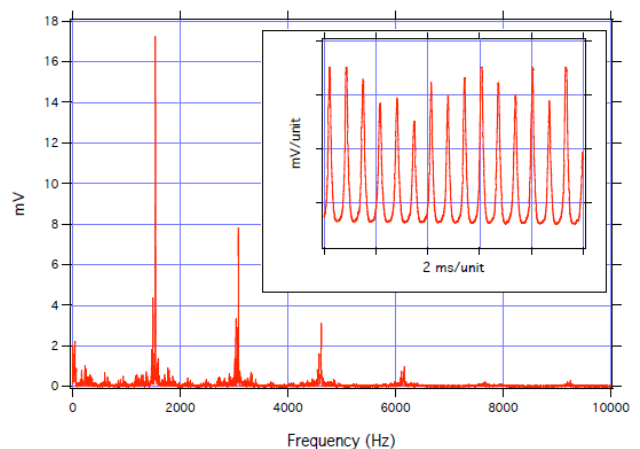


Figure 7: bursts of coherent THz at 183 μA bunch current.

REFERENCES

- [1] D. Robin et al., “Low alpha experiments at the ALS”, Internal report LBL-37802, Berkeley, 1995.
- [2] J. Feikes, K. Holldack, P. Kuske, G. Wüstefeld, “Sub-picosecond bunches in the BESSY storage ring”, EPAC’04, Lucerne, June 2004, p. 1954.